

MEASUREMENT RESULTS OF THE IMPEDANCE OF THE RF-CAVITY AT THE RCS IN J-PARC

Y. Shobuda, H. Harada, H. Hotchi, J-PARC Center, Ibaraki, Japan

Abstract

The kicker impedance dominates at the RCS in J-PARC. Recently, we observe beam instabilities, which are not explained by the kicker. As a candidate causing the beam instability, the impedance of the RF-cavity is measured. The longitudinal impedance is measured by stretching a single-wire inside the cavity. On the other hand, the measurement of the transverse impedance is done by horizontally shifting the single-wire, due to the accuracy problem. The measured impedance is too low to explain the beam instability.

INTRODUCTION

The Rapid Cycling Synchrotron (RCS) in Japan Proton Accelerator Research Complex (J-PARC) [1] is a machine, where protons are accelerated from 400 MeV to 3 GeV during 20 ms. The injection beam from the LINAC is accumulated there during 500 μ s in synchronization with the excitation of the injection bump magnets [2].

The role of the RCS is to deliver the proton beam to the Material and Life Science Facility (MLF)-target as well as to work as the injector to the main ring in J-PARC. Main objective of the RCS is to routinely supply one mega-watt beam (8.3×10^{13} particles per a pulse with the repetition rate 25 Hz) to the MLF-target.

Let us consider a situation that 8.3×10^{13} particles per a pulse are accelerated, where the chromaticity is corrected only at the injection energy. When the bunching factor of the beam and the tune-tracking are inadequately manipulated during the ramping process [3], we can observe beam instabilities [4]. However, the characteristic of the beam behavior can be understood by assuming that the cause of the instability mainly attributes to the kicker impedance. In this sense, the RCS is characterized by the machine where the kicker impedance dominates, from an impedance point of view [3–7].

At the high intensity proton beam, the space charge effects produce large tune spreads. Thereby, some particles cross resonance lines, which are the source of the particle losses. In order to avoid the particle loss, the typical horizontal and the vertical operation tunes of the RCS are chosen to be $\nu_x = 6.45$ and $\nu_y = 6.42$, respectively, at the injection period [8].

To make matters worse, the resonance lines severely restrict the allowable operation region near the present tunes ($\nu_x = 6.45, \nu_y = 6.42$) at the RCS. Accordingly, a trial was done to change the operation tunes to the other ones ($\nu_x = 5.86, \nu_y = 5.86$). This is because significant resonance structures cannot exist there from a viewpoint of magnetic error sources.

5: Beam Dynamics and EM Fields

Contrary to our expectations, significant beam instabilities are observed under the operation tunes.

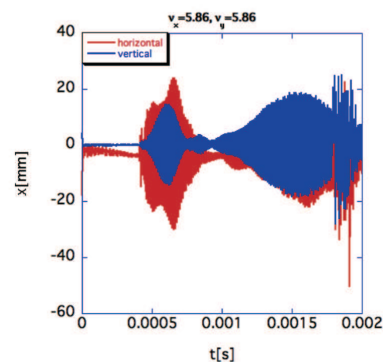


Figure 1: Beam instability observed at $\nu_x = \nu_y = 5.86$.

The measured results are shown in Fig. 1. The horizontal and the vertical axes show the acceleration period and the transverse position of the beam, respectively. The red and the blue lines show the horizontal and the vertical beam positions, respectively. The chromaticity is corrected only at the injection energy by quarter against the full chromaticity correction. The particle per a bunch is only 1.32×10^{13} , which is equivalent to 316 kW beam. Considering 1MW-equivalent beam is already achieved at the RCS [8], the impedance source is incredibly huge. To tell the truth, the beam power is weaker and the conditions (partial correction of the chromaticity) may rather stabilize the beam.

The results in Fig. 1 demonstrate that the beam becomes unstable around 1.5 ms. However, the injection bump magnets are perfectly turned off at that time. Consequently, it is hard to consider that the instability attributes to the field errors due to the injection bump magnet [9, 10]. Moreover, the beam instability is not related to x - y coupling, because the instability occurs even when one of the transverse tunes sits on $\nu_x = 5.86$ or $\nu_y = 5.86$ lines, independently.

Now, it is necessary to review the impedance source causing the unexpected beam instabilities, and to specify the impedance source along the RCS. As a first step, let us measure the impedance of RF-cavity. In the next section, let us see the measurement scheme and the results.

MEASUREMENTS

A schematic picture of RF-cavity is shown in Fig. 2. Four chambers are connected through three ceramic breaks (red). The chambers are surrounded over six Magnetic Alloy cores (blue). The inner radius of the chamber is 123.5 mm.

Content from this work may be used under the terms of the CC BY 3.0 licence (© 2015). Any distribution of this work must maintain attribution to the author(s), title of the work, publisher, and DOI.

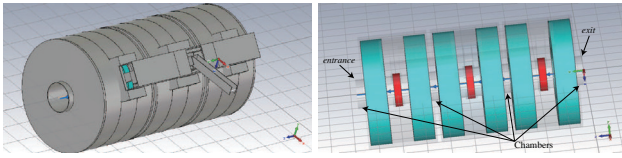


Figure 2: A schematic picture of RF-cavity (described by using CST [11]). The left and the right figures show the overview and the inner view of the cavity, respectively.

The standard wire methods well-describe the beam impedances [12, 13]. The longitudinal impedance is measured by stretching a copper coated piano wire with the radius $80\mu\text{m}$ in the cavity. The impedance is obtained by using the standard log-formula [12, 13]:

$$Z_L^{mes} = -2Z_{cc} \log \frac{S_{21}^{cavity}}{S_{21}^{ref}}, \quad (1)$$

where Z_{cc} ($\approx 440.5 \Omega$ in our case) is the characteristic impedance for the coaxial-structure made by the wire and the chambers, S_{21}^{cavity} and S_{21}^{ref} are the transmission coefficient for the cavity, and one where the cavity is replaced by the reference (aluminum) chamber, respectively. The distance between the entrance/exit of the cavity and the edge of the nearest ceramic breaks is 323 mm. Accordingly, we decide that the fixtures for the wire are attached on both the entrance and the exit of the cavity, directly.

The transmission coefficients S_{21}^{cavity} and S_{21}^{ref} are measured with 4-port Agilent Technologies ENA Series Network Analyzer E5071C [14]. The calibration is done by 2-port electric calibration module 85092C. The measurement is done by sweeping the frequency of the input signal (the sinusoidal function with single-frequency). The averaging factor is 100.

Based on the definition of the transverse impedances, the transverse impedance should be measured by stretching twin-wires and by observing the transmission coefficients for the differential mode. However, the accuracy problems made us face the difficulty of the precise measurement by the method. In this report, let us confine our discussion to the transverse impedances obtained through the longitudinal impedance measured by the single wire method.

Concretely, let us prepare for the fixtures for the wire whose position x_w can arbitrarily move in the horizontal direction. By using the fixtures, once the longitudinal impedance is measured for the different wire-position x_w , the transverse impedance is obtained by detecting the wire positions x_w dependence of the longitudinal impedance [15]. The formula is given by

$$Z_T^{mes} = \frac{1}{2k} \frac{\partial^2 Z_L^{mes}}{\partial x_w^2}, \quad (2)$$

where k is wave number. The position of the wire moves from -70 mm to 70 mm. The longitudinal impedance is measured at intervals of 10 mm in the range.

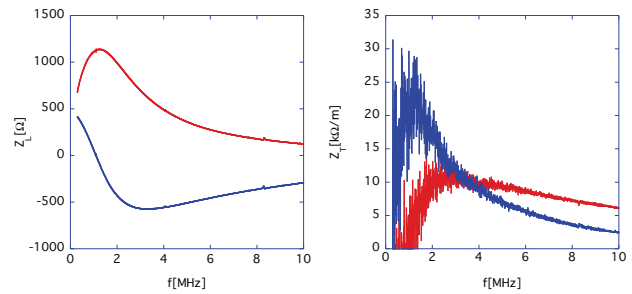


Figure 3: The measurement results of the longitudinal (left) and the transverse (right) impedances. The red and the blue lines show the real and the imaginary parts of the impedances, respectively.

The measurement results are shown in Fig. 3. The left and the right figures show the longitudinal (for $x_w = 0$) and the transverse impedances, respectively. The red and the blue lines show the real and the imaginary parts of the impedances, respectively.

In the RCS, twelve cavities and eight kickers are installed. Now, we can estimate the total contribution from the impedance source to the RCS. The results are shown in Fig. 4. The left and the right figures show the real and the imaginary parts of the impedance. The red lines show the contribution only from the kickers to the impedance, while the blue lines show the total contribution including the cavities. Consequently, we find that the cavity impedances significantly deform the impedance where we only consider the kicker contributions.

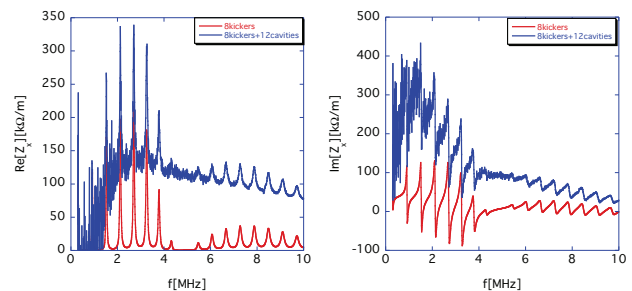


Figure 4: Contributions from the eight kickers' impedance and the twelve cavities' one to the RCS impedance.

ESTIMATION OF THE CAVITY IMPEDANCE IMPACT TO THE RCS

Here, let us estimate the impact on the RCS by the addition of the cavity impedance to the total impedance. First, let us investigate whether the transverse microwave instabilities cause the beam instability shown in Fig. 1.

The criterion is derived in [16], which is expressed as

$$|Z_{x,y}((n - \nu_{x,y})\omega_0)| < 4 \frac{E_0}{e} \frac{\nu_{x,y}}{I_p R} \left(\frac{\Delta p}{p} \right)_{FWHM} \cdot F S_{x,y}, \quad (3)$$

where

$$S_{x,y} = |(n - \nu_{x,y})\eta + \nu_{x,y}\xi_{x,y}|, \quad (4)$$

n is integer, I_p is the peak current, η is the slippage factor, R is the average radius of the RCS, E_0 is the beam energy, F is the form factor, $\nu_{x,y}\xi_{x,y}$ is the chromaticity in the transverse direction, and $(\Delta p/p)_{FWHM}$ is full width of half maximum of the momentum spread of the beam.

We have already known that the beam instability does not occur for one megawatt beam around the Lorentz- $\beta = 0.737$, if the chromaticity is corrected only at the injection energy. Considering the phenomenon, the form factor F may be evaluated as around ten. Roughly, let us assume $F = 10$.

As we see Eq.(3), we find that the stability condition depends on the tunes and the chromaticity. Here, both the horizontal and the vertical tunes are chosen to be $\nu_x = \nu_y = 5.86$, respectively. Moreover, both the horizontal chromaticity and the vertical one are evaluated as -5.23 and -5.86 at the Lorentz- $\beta = 0.737$, respectively, because the chromaticity is corrected by quarter at the injection energy, in Fig. 1. The results are shown by the red line in Fig. 5. The blue line shows the critical line given by Eq.(3), below which the beam becomes stable. The partial correction of the chromaticity ensures the stability region.

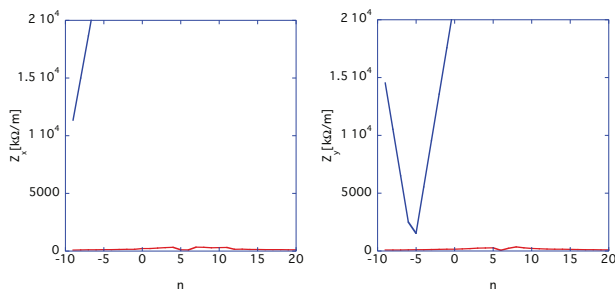


Figure 5: Stability condition for 316 kW beam.

The coupled bunch instability may be suspected to cause the beam instability at $\nu_x = \nu_y = 5.86$. Indeed, that causes the beam instability observed for one megawatt (or 750 kW)-equivalent beam, when the tunes are chosen to be $\nu_x = 6.45$ and $\nu_y = 6.42$ at the injection energy. The characteristic of the instability is that it is observed after about 10 ms during the acceleration period, when the chromaticity is corrected only at the injection energy, the choice of the bunching factor and the tune manipulation are inadequate. In the lower energy region, the space charge effects suppress the beam instability. If the same damping mechanism works on $\nu_x = \nu_y = 5.86$, 316 kW beam is sufficiently stabilized, as well.

SUMMARY

The cavity impedance of the RCS in J-PARC is measured by the wire method. Though the cavity impedances significantly contribute the total impedance of the RCS, it is too low to explain the beam instability observed for 316 kW beam with $\nu_x = \nu_y = 5.86$.

REFERENCES

- [1] <http://j-parc.jp/index-e.html>
- [2] I. Sakai *et al.*, ‘H⁻ painting injection system for the J-K 3-GeV high-intensity proton synchrotron’, EPAC2002, Paris, France, 1040, (2002)
- [3] Y. Shobuda *et al.*, ‘The kicker impedance and its effect on the RCS in J-PARC’, HB2014, East-Lansing, Michigan, USA, THO2AB02, (2014)
- [4] A. W. Chao, *Physics of collective beam instabilities in high energy accelerators*, (Wiley, New York, 1993).
- [5] Y. H. Chin *et al.*, ‘Impedance and beam instability issues at J-PARC rings’, HB2008, Nashville, Tennessee, WGA01-1, (2008)
- [6] Y. Shobuda *et al.*, ‘A trial to reduce the kicker impedance of 3-GeV RCS in J-PARC’, IPAC2013, Shanghai, China, 1742, (2013)
- [7] Y. Shobuda *et al.*, ‘Measurement scheme of kicker impedances via beam-induced voltages of coaxial cables’, Nuclear Instruments and Methods A **713**, 11, 52-70, (2013)
- [8] H. Hotchi, ‘Space Charge Induced Beam Loss and Mitigation in the J-PARC RCS’, Space-Charge 2015, Trinity College, Oxford, (2015)
- [9] Y. Shobuda *et al.*, ‘Analytical method for the evaluation of field modulation inside the rf-shielded chamber with a time-dependent dipole magnetic field’, Phys. Rev. ST Accel. Beams, **12**, 032401, (2009)
- [10] Y. Shobuda *et al.*, ‘Analytical Estimation of the Field Modulation during the Injection Period of the 3 GeV RCS in J-PARC’, to be published in *J-PARC symposium*, (2015)
- [11] <https://www.cst.com/>
- [12] *Handbook of Accelerator Physics and Engineering*, ed. A. W. Chao and M. Tigner, (1999)
- [13] H. Hahn, ‘Validity of coupling impedance bench measurements’, Phys. Rev. ST Accel. Beams **3**, 122001, (2000)
- [14] <http://www.home.agilent.com/>
- [15] G. Nassibian and F. Sacherer, ‘Methods for Measuring Transverse Coupling Impedances in Circular Accelerators’, NIM **159**, 21, (1979)
- [16] K. Y. Ng, Chapter 14 in FERMILAB-TM-2169, Proton driver study. II. (Part 1) G.W. Foster *et al.* (ed.), (Fermilab), (2002)